Acta Pharmaceutica Sinica B 2012;2(1):53–59

Institute of Materia Medica, Chinese Academy of Medical Sciences
Chinese Pharmaceutical Association

Acta Pharmaceutica Sinica B

www.elsevier.com/locate/apsb
www.sciencedirect.com

ORIGINAL ARTICLE

Spectroscopic and dynamic light scattering studies of the interaction between pterodontic acid and bovine serum albumin

Yunfang Li, Guangzhong Yang, Zhinan Mei*

College of Pharmacy, South Central University for Nationalities, Wuhan 430074, China

Received 31 August 2011; revised 8 October 2011; accepted 6 December 2011

KEY WORDS

Pterodontic acid;
Bovine serum albumin;
Fluorescence quenching;
Synchronous fluorescence;
Three-dimensional fluorescence;
Dynamic light scattering

Abstract Pterodontic acid (PA) has been isolated from *Laggera pterodonta*, a Chinese herbal medicine, and shown to possess antibacterial activity *in vitro*. To facilitate its preclinical development, the interaction between PA and bovine serum albumin (BSA) was studied using a fluorescence quenching technique, ultraviolet–visible spectrophotometry and dynamic light scattering (DLS). At temperatures of 297 K and 310 K and an excitation wavelength of 282 nm, the fluorescence intensity of BSA decreased significantly with increasing concentration of PA attributed to the formation of a PA–BSA complex. The apparent binding constant, number of binding sites and corresponding thermodynamic parameters were calculated and the main intermolecular attraction shown to result from hydrogen bonding and van der Waals forces. Synchronous fluorescence spectrometry revealed that the binding site in the complex approached the microenvironment of Trp and three-dimensional fluorescence spectroscopy showed the binding induced conformational changes in BSA. Using DLS, increasing PA concentration was shown to cause a gradual increase in hydrodynamic diameter and significant aggregation of the complex.

*Corresponding author. Tel.: +86 27 67843713; fax: +86 27 67841196.
E-mail address: meizhinan@163.com (Zhinan Mei).

Peer review under responsibility of Institute of Materia Medica, Chinese Academy of Medical Sciences and Chinese Pharmaceutical Association.
doi:10.1016/j.apsb.2011.12.001

1. Introduction

Serum albumin is the most abundant protein in the circulatory system and the major macromolecule contributing to the osmotic blood pressure[1]. The most important function of albumin is to serve as a depot and transport protein for a variety of compounds such as fatty acids, amino acids, hormones, bilirubin, drugs and pharmaceuticals[2]. The knowledge of the interaction between drug molecules and serum albumin is useful in interpreting the pharmacokinetics and transport of a drug. The structural and energetic aspects of the interaction provide a rational basis for a fundamental understanding of the interaction and the further development of an efficient therapeutic agent[3–5].

Pterodontic acid[6,7] (PA, Fig. 1) is a eudesmane sesquiterpene isolated from *Laggera pterodonta* (DC.) Benth. which is widely distributed in Yunnan, China, and is used as a folk medicine[8]. Sesquiterpenes are a large category of compounds with many pharmacological effects due to possessing antitumor[9], antibacterial[10,11], anti-inflammatory[12] and anti-allergic activities[13]. Some eudesmane sesquiterpenes isolated from *L. pterodonta* show cytotoxicity towards tumor cells[14] and antibacterial activity[15]. Previous studies in our laboratory also showed that PA possesses antibacterial activity *in vitro*[16]. Due to this wide ranging pharmacological activity, it is appropriate to investigate the interaction of PA with protein as part of its preclinical development. Bovine serum album (BSA) is selected as a model protein because of its structural homology with human serum albumin (HSA)[17]. The present paper reports the results of an investigation of the interaction between PA and BSA by spectroscopic techniques (fluorescence, UV–vis absorption, synchronous fluorescence, 3D fluorescence) and dynamic light scattering (DLS).

2. Materials and methods

2.1. Apparatus and reagents

All fluorescence measurements were carried out in 1.0 cm quartz cells on an LS55 recording spectrophotometer (Perkin Elmer Corporation, USA) equipped with a thermostatted circulating water bath. All UV–vis spectra were recorded on a Lambda35 recording spectrophotometer (Perkin Elmer Corporation, America). DLS was performed on a laser scattering spectrometer (BI 200SM, Brookhaven Instruments Corporation, USA) equipped with a digital correlator (BI-TurboCorr). All pH measurements were made using a pHs-3 digital pH-meter (Shanghai Lei Ci Device Works, Shanghai, China) with a combined glass electrode.

BSA was purchased from Sigma Chemical Company and a BSA stock solution (5×10^{-5} M) was prepared in Tris–HCl (0.05 M) pH 7.4 buffer solution containing 0.1 M NaCl. PA was isolated from *L. pterodonta* (DC.) Benth. in our laboratory and its structure confirmed by comparison of its ^{1}H NMR and ^{13}C NMR spectra with reference spectra[16]. A PA solution (9.0×10^{-3} M) was prepared in methanol. All other reagents were of analytical grade and used as received. Doubly-distilled water was used in all experiments and solutions were stored at 4 °C when not in use.

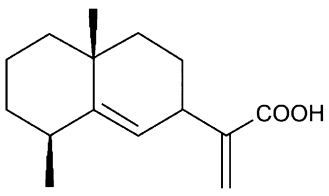

Figure 1 Chemical structure of pterodontic acid (PA).

2.2. Experimental methods

Fluorescence measurements were carried out in 1.0 cm quartz cells by successively adding from a micro-injector 10 μL aliquots of the PA (9.0×10^{-3} M) solution to 3.0 mL BSA (1×10^{-6} M) solution. The total volume of PA solution added (60 μL) was small compared to the total volume[5]. Fluorescence emission spectra in the range 300–500 nm were measured at an excitation wavelength of 282 nm. All experiments were performed at two temperatures (297 K and 310 K).

The UV–vis absorption spectra of BSA in the absence and presence of PA were recorded at 297 K in the range 200–400 nm. In order to exclude the contribution from PA absorption, equal concentrations of PA were present in the reference cell.

The synchronous fluorescence characteristics of PA–BSA were measured at 297 K using different values of $\Delta\lambda$ ($\Delta\lambda = \lambda_{ex} - \lambda_{em}$). For $\Delta\lambda = 15$ nm, the spectral characteristics of protein tyrosine (Tyr) residues were evident while for $\Delta\lambda = 60$ nm, the spectral characteristics of protein tryptophan (Trp) residues were observed.

Three-dimensional fluorescence spectra of BSA were recorded in the presence and absence of PA with an excitation wavelength in the range 200–390 nm and an emission wavelength in the range 200–500 nm.

DLS measurements were made at 297 K with a scattering angle of 90° and a sampling time in the range 0.005–100 ms. The results were analyzed using the Non Negative Least Square (NNLS) method[18]. All solutions were clarified by ultrafiltration through 0.2 μm filters (Millipore Corporation, USA). The titration involved successive additions of the 9×10^{-3} M solution of PA in methanol to 3.0 mL of a 5×10^{-6} M BSA solution (pre-equilibrated at 297 K for 20 min) to give a final PA concentration of 2.4×10^{-4} M. Three or more measurements were performed after each addition to check repeatability.

3. Results and discussion

3.1. Mechanism of the BSA–PA interaction

Protein is a fluorescent substance due to the presence of the amino acids Trp, Tyr and phenylalanine (Phe). PA acts as a fluorescence quencher of BS as shown in Fig. 2, which displays the emission spectra of BSA in the presence of increasing concentrations of PA at 297 K and 310 K. As the data shows, an excitation wavelength of 282 nm produces a strong emission band at 350 nm, which decreases uniformly at the two temperatures when PA is added. In addition, the wavelength of maximum BSA fluorescence shifts from 350 to 343 nm at 297 K and from 351 to 346 nm at 310 K implying the microenvironment around the BSA chromophore changes in the presence of PA.

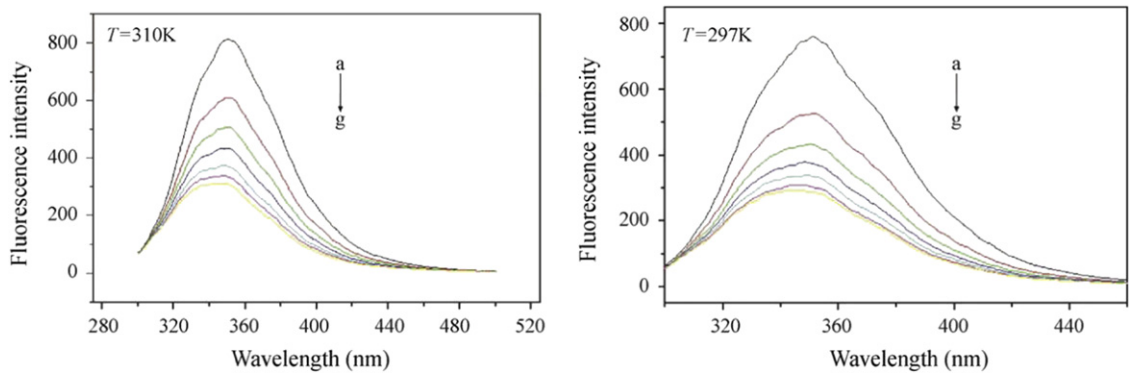

Figure 2 Fluorescence emission spectra of PA–BSA system excited at 282 nm (pH = 7.40, T = 297 K and 310 K). (a) BSA at 1×10^{-6} M; (b–g) BSA at 1×10^{-6} M in the presence of PA at 3.0×10^{-5}, 6.0×10^{-5}, 9.0×10^{-5}, 12.0×10^{-5}, 15.0×10^{-5} and 18.0×10^{-5} M, respectively.

In order to investigate the quenching mechanism, the fluorescence quenching data were analyzed by the Stern–Volmer equation[19]:

$$F_0/F = 1 + K_{sv}[Q] = 1 + K_q\tau_0[Q] \quad (1)$$

where F_0 and F are the fluorescence intensities of protein in the absence and presence of the quencher, respectively, K_q is the quenching rate constant, K_{sv} is the Stern–Volmer constant, τ_0 is the average lifetime of the molecule without quencher (1×10^{-8} s for BSA[20]) and [Q] is the quencher concentration. In general, quenching is classified as either dynamic or static. Dynamic quenching is collisional quenching which is enhanced by increasing temperature but diminished by increasing viscosity. A higher temperature results in faster diffusion and a higher value of K_{sv}. Static quenching results from the formation of a stable non-fluorescent complex between the fluorophore and the quencher. In this case, a higher temperature reduces the stability of the complex and leads to a lower value of K_{sv}.

A Stern–Volmer plot of the data is shown in Fig. 3 and the calculated K_{sv} values at the two temperatures are given in Table 1. The results show that K_{sv} and K_q decrease with increasing temperature indicating a static quenching mechanism. In addition, the values of K_q were greater than the maximum scatter collisional quenching constant (2.0×10^{10} M/s)[21], which further indicates that the probable quenching mechanism involves complex formation rather than dynamic collisions.

UV–vis absorption spectroscopy is used to explore structural changes in proteins and to investigate protein-small molecule interactions. BSA has two main absorption bands, one at 200–230 nm arising from the polypeptide backbone, and one at 260–300 nm due to the aromatic amino acids (Trp, Tyr and Phe)[22]. According to the principles of absorption spectroscopy, dynamic quenching is induced only by excited fluorescent molecules such that absorption spectra of florescent substances are not generally affected by the addition of a quencher. In contrast, static quenching is induced by the formation of ground-state complexes such that absorption spectra are changed to a greater or lesser extent[23].

The UV–vis absorption spectra of PA and BSA are given in Fig. 4 where it is seen that PA and BSA possess maximum absorption (λ_{max}) at 207 and 206 nm, respectively. The absorption spectra of the PA–BSA complex show a decrease in the intensity of the absorption peak of BSA with a slight shift in the λ_{max} from 206 to 210 nm with the addition of PA. However, the absorption peak at 278 nm shows no obvious change. The results indicate that quenching is mainly a static process and that at least one PA–BSA complex is probably formed[24]. The polarity of the microenvironment of BSA is altered leading to a conformational change where the peptide strands of BSA are extended and its hydrophobicity is decreased.

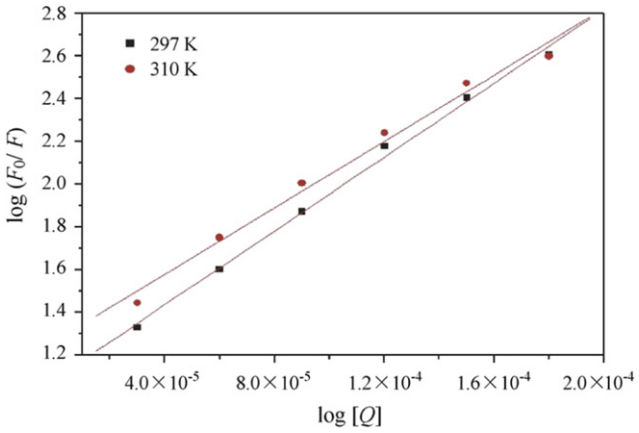

Figure 3 Stern–Volmer plot for the PA–BSA system at two temperatures ($C_{BSA} = 1 \times 10^{-6}$ M, λ_{ex} = 282 nm; pH = 7.40).

Table 1 Stern–Volmer quenching constants at two temperatures.

T (K)	K_{sv} (10^3 L/mol)	K_q (10^{11} L/mol/s)	R	SD
297	8.647	8.647	0.99797	0.03464
310	7.776	7.776	0.99344	0.05617

R: correlation coefficient; SD: standard deviation.

3.2. *Calculation of binding parameters*

For a static quenching interaction, the experimental data can be processed using the following formula:

$$\log(F_0/F - 1) = \log K_A + n\log[Q] \quad (2)$$

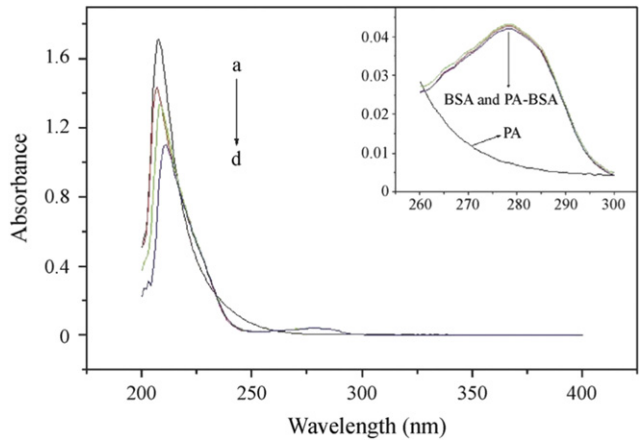

Figure 4 Ultraviolet–visible absorption spectra (pH = 7.40, T = 297 K) of (a) PA at 1.8×10^{-4} M; (b) BSA at 1×10^{-6} M; (c and d) BSA at 1×10^{-6} M in the presence of PA at 9.0×10^{-5} and 18.0×10^{-5} M, respectively.

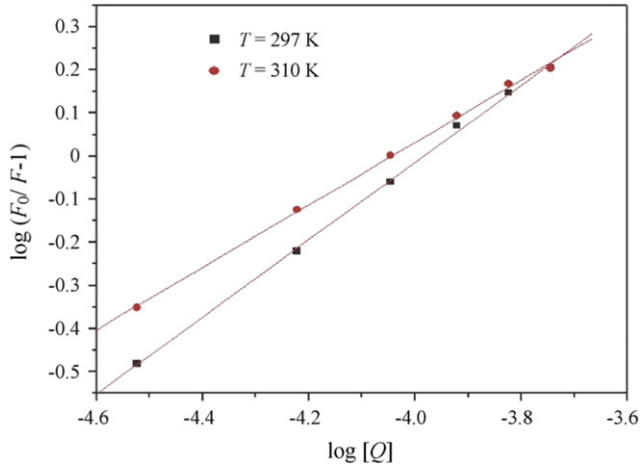

Figure 5 Plot of $\log(F_0/F-1)$ vs. $\log[Q]$ at two temperatures ($C_{BSA} = 1 \times 10^{-6}$ M, λ_{ex} = 282 nm; pH = 7.40).

Table 2 Binding parameters of PA–BSA at two temperatures.

T (K)	K_A (10^3 L/mol)	n	R	SD
297	3.728	0.89647	0.99946	0.00947
310	0.852	0.72472	0.99927	0.00894

R: correlation coefficient; SD: standard deviation.

where F_0, F and $[Q]$ are the same as in Eq. (1), n is the number of binding sites and K_A is the binding constant. Fig. 5 shows the plots of $\log(F_0/F-1)$ vs. $\log[Q]$ for the PA–BSA system at the two temperatures and Table 2 presents the calculated results. The results show that K_A decreases as temperature increases, which probably indicates the formation of a compound partially decomposes at higher temperature. The value of n is equal to approximately 1 indicating the involvement of a single binding site in the PA–BSA interaction.

3.3. *Thermodynamic analysis and intermolecular forces*

The intermolecular forces of interaction between a small molecule and a biomolecule mainly include hydrogen bonding, van der Waals forces, electrostatic forces and hydrophobic forces. Within a small temperature range, the enthalpy of interaction can be regarded as constant leading to the following equations:

$$\ln(K_{A2}/K_{A1}) = \Delta H(1/T_1 - 1/T_2)/R \quad (3)$$

$$\Delta G = \Delta H - T\Delta S \quad (4)$$

$$\Delta S = -(\Delta G - \Delta H)/T \quad (5)$$

where R is the gas constant, T is the absolute temperature and K_A is the apparent binding constant at the corresponding temperature T. If $\Delta S > 0$ and $\Delta H > 0$, the main force of interaction is the hydrophobic force; if $\Delta S > 0$, $\Delta H < 0$, the main force is electrostatic attraction; if $\Delta S < 0$, $\Delta H < 0$, the main force includes both van der Waals forces and hydrogen bonding[25]. Table 3 shows the values of ΔH, ΔS and ΔG at the two temperatures. The negative values of ΔG reveal that the interaction process is spontaneous. The fact that $\Delta S < 0$ and $\Delta H < 0$ indicates that the interaction between PA and BSA is mainly due to hydrogen bonding and van der Waals forces.

3.4. *Synchronous fluorescence spectroscopy*

Synchronous fluorescence spectroscopy is frequently used to characterize the interaction between a quenching agent and a protein since it provides information about the molecular environment in the vicinity of the chromosphere. It has several advantages including high sensitivity, spectral simplicity, spectral bandwidth reduction and resistance to perturbing effects[26]. As shown in Fig. 6, PA has little effect on the fluorescence intensity of Tyr ($\Delta\lambda$ = 15 nm) but significantly decreases that of Trp ($\Delta\lambda$ = 60 nm) suggesting that PA binding to BSA affects the microenvironment of Trp but not that of Tyr. However, no obvious wavelength shift is observed for both Tyr and Trp as the PA concentration is increased.

3.5. *Three-dimensional fluorescence spectroscopy*

Application of the three-dimensional fluorescence technique has become popular in recent years because it allows fluorescence characteristics to be acquired by changing the excitation and emission wavelengths simultaneously. Fig. 7 displays three-dimensional fluorescence spectra of BSA in the absence and presence of PA and corresponding spectral parameters are presented in Table 4. Fig. 7 shows two typical fluorescence peaks (I and II): Peak I at 280 nm mainly reveals the spectral behavior of the Trp and Tyr residues since excitation of BSA at this wavelength mainly reveals their intrinsic fluorescence;

Table 3 Thermodynamic parameters of the PA–BSA interaction.

T (K)	ΔH (kJ/mol)	ΔS (J/mol/K)	ΔG (kJ/mol)
297	−86.86	−224.07	−20.31
310	−86.86	−224.10	−17.39

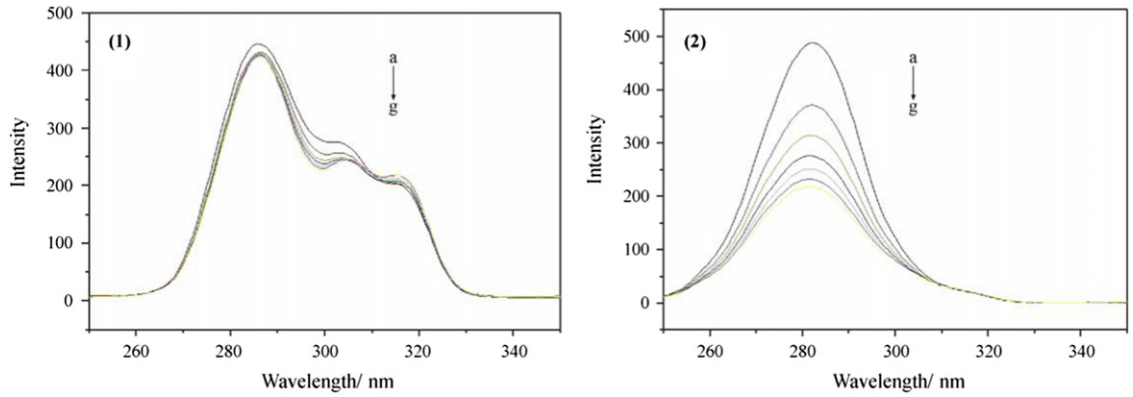

Figure 6 Synchronous scanning fluorescence spectra of the PA–BSA system. (1) $\Delta\lambda = 15$ nm; (2) $\Delta\lambda = 60$ nm. (a) BSA at 1×10^{-6} M; (b–g) BSA at 1×10^{-6} M in the presence of PA at 3.0×10^{-5}, 6.0×10^{-5}, 9.0×10^{-5}, 12.0×10^{-5}, 15.0×10^{-5} and 18.0×10^{-5} M, respectively.

Table 4 Three-dimensional fluorescence spectral parameters of BSA alone and in the presence of PA.

System	Peak I (nm, $\lambda_{ex}/\lambda_{em}$)	$\Delta\lambda$ (nm)	Intensity	Peak II (nm, $\lambda_{ex}/\lambda_{em}$)	$\Delta\lambda$ (nm)	Intensity
BSA	280/352	72	347.46	230/352	122	489.77
PA–BSA	280/347	67	180.91	230/348	118	209.71

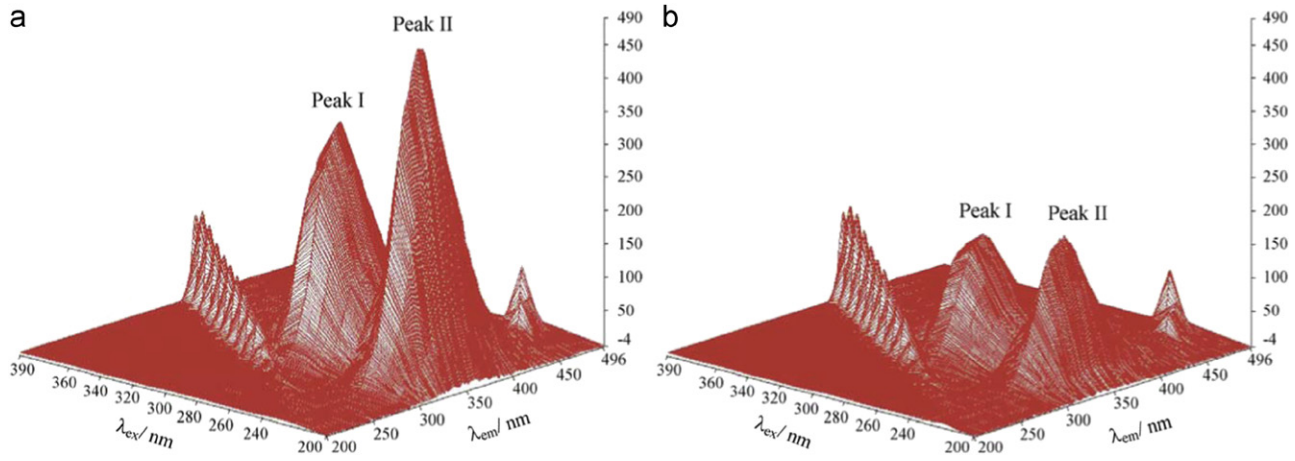

Figure 7 Three-dimensional fluorescence spectra of (a) BSA at 1×10^{-6} M; (b) BSA at 1×10^{-6} M, PA at 9×10^{-5} M (pH = 7.40; $T = 297$ K).

peak II at 230 nm mainly reflects the fluorescence of the polypeptide backbone of BSA[27]. Quenching of fluorescence of BSA by PA involved both peaks but to a different degree. The decrease in the fluorescence intensity of these peaks in combination with the changes in synchronous fluorescence and UV–vis absorption indicate that the interaction of PA with BSA induces a secondary structural change in the BSA molecule.

3.6. *Dynamic light scattering*

DLS is a powerful technique that yields important structural information about biological macromolecules in solution[28,29]. It makes it possible to measure the hydrodynamic diameter, polydispersity and presence of aggregates in proteins. In fact, monitoring the size of a protein in the presence of a drug is one way to investigate their interaction[30,31]. As shown in Fig. 8, the hydrodynamic diameter of BSA increased from 7.3 to 22.8 nm with increasing PA concentration as did the scattered light intensity of BSA. On this basis, it can be inferred that a PA–BSA complex forms and aggregates as the PA concentration increases. This inference was confirmed through studies of the size distribution of BSA (Fig. 9a) and the PA–BSA complex (Figs. 9b–e). Whilst a few dimers (13.5 nm) of BSA are present in Tris–HCl buffer (pH 7.4) together with BSA itself (6.6–7.9 nm), addition of PA causes formation of aggregates with size increasing from 17.9 to 21.4 nm (Fig. 9b) to 63.6–122.8 nm (Fig. 9e). These results imply that the binding between PA and BSA leads to a conformational change in BSA which contributes to the aggregation of the PA–BSA complex.

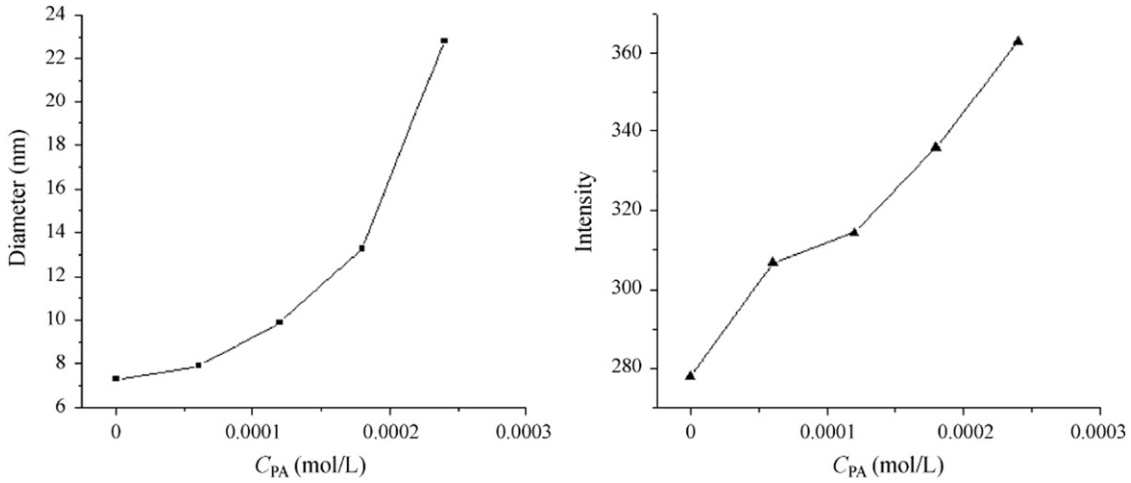

Figure 8 The PA concentration dependence of the hydrodynamic diameter and scattered light intensity of BSA (pH = 7.40, $T = 297$ K) $C_{PA} = 0$, 6.0×10^{-5}, 12.0×10^{-5}, 18.0×10^{-5} and 24.0×10^{-5} M.

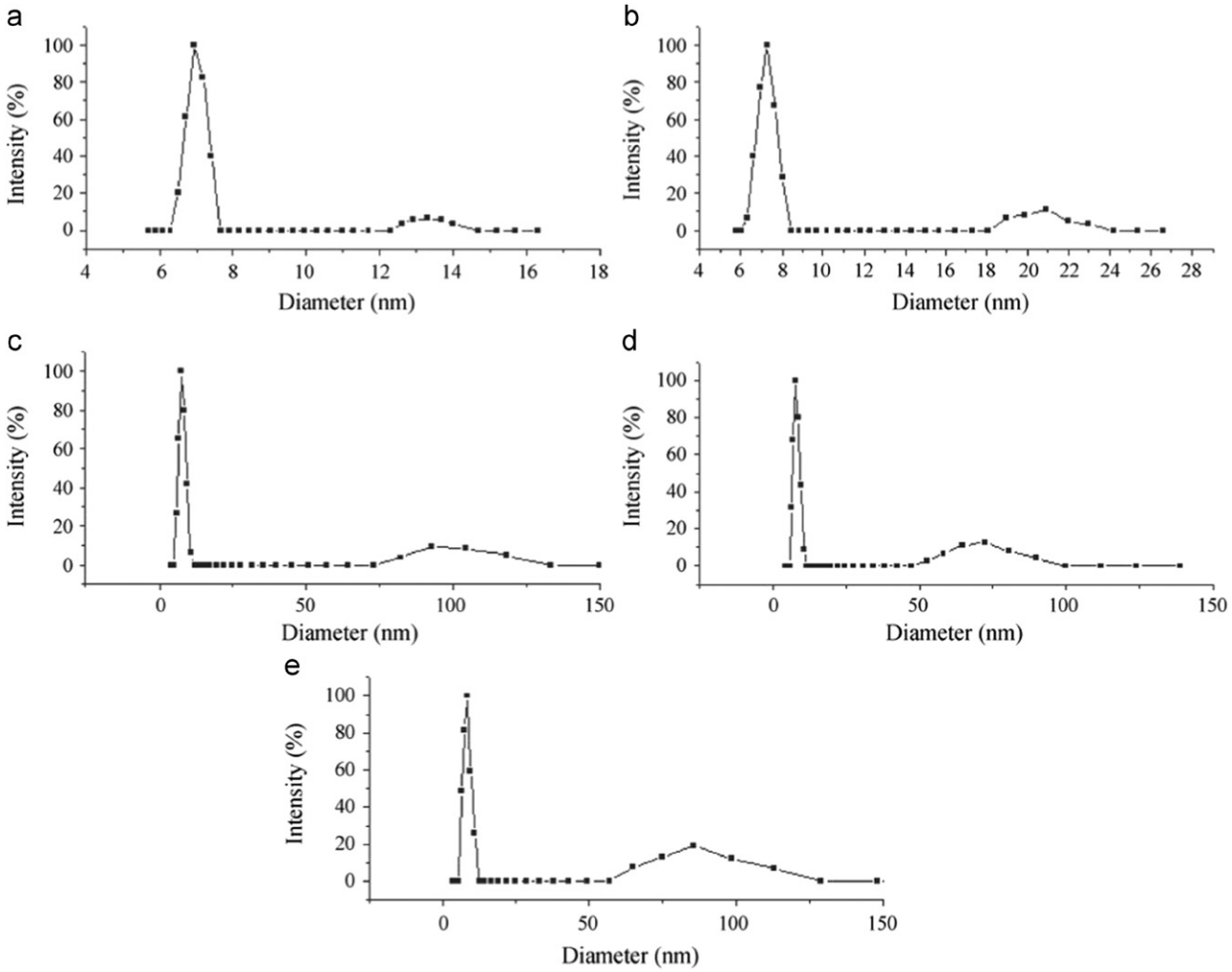

Figure 9 Size distribution of (a) BSA and (b–e) the PA–BSA complex (pH = 7.40, $T = 297$ K). (a–e) BSA at 5×10^{-5} M in the presence of PA at 0, 6.0×10^{-5}, 12.0×10^{-5}, 18.0×10^{-5} and 24.0×10^{-5} M, respectively.

4. Conclusions

The present paper describes an investigation of the mechanism of interaction between PA and protein using spectroscopic techniques and DLS. PA quenches the fluorescence of BSA through a static quenching mechanism. Bonding constants and the number of binding sites were determined and hydrogen bonding and van der Waals forces were shown to be the main source of intermolecular attraction. UV–vis, synchronous fluorescence and three-dimensional fluorescence studies revealed the interaction leads to a change in the secondary structure of BSA, a result supported by DLS studies. Overall it was shown that PA not only binds to BSA but also induces aggregation of the PA–BSA complex. This information will assist in understanding the behavior of PA *in vivo* and contribute to its preclinical development.

Acknowledgment

This work was supported by the Special Fund for Basic Scientific Research of Central Colleges, South-Central University for Nationalities (No. CZQ11013) and by the Wuhan Science and Technology Bureau (No. 201051730558).

References

1. Carter DC, Ho JX. Structure of serum albumin. *Adv Protein Chem* 1994;**45**:153–203.
2. Olson RE, Christ DD. Plasma protein binding of drugs. *Ann Rep Med Chem* 1996;**31**:327–36.
3. Ge F, Jiang L, Liu D, Chen C. Interaction between alizarin and human serum albumin by fluorescence spectroscopy. *Anal Sci* 2011;**27**:79–84.
4. Sandhya B, Hegde AH, Kalanur SS, Katrahalli U, Seetharamappa J. Interaction of triprolidine hydrochloride with serum albumins: thermodynamic and binding characteristics, and influence of site probes. *J Pharm Biomed Anal* 2011;**54**:1180–6.
5. Tang D, Li HJ, Li P, Wen XD, Qian ZM. Interaction of bioactive components caffeoylquinic acid derivatives in Chinese medicines with bovine serum albumin. *Chem Pharm Bull (Tokyo)* 2008;**56**: 360–5.
6. Mei ZN, Li YF, Yu X, Yang GZ. Pterodontic acid. *Acta Crystallogr E* 2006;**62**:1841–3.
7. Li SL, Ding JK. Four new sesquiterpenoids from *Laggera pterodonta*. *Acta Bot Yunnan* 1996;**18**:349–52.
8. Jiangsu New Medical College. *A dictionary of a traditional Chinese drugs*. Shanghai: Sciences and Technology Publishing House; 1977. p. 1889–90.
9. Moon HI, Zee O. Anticancer activity of sesquiterpene lactone from plant food (*Carpesium rosulatum*) in human cancer cell lines. *Int J Food Sci Nutr* 2011;**62**:102–5.
10. Semwal S, Sharma RK. Antibacterial sesquiterpene lactone glucoside from seed pods of *Bauhinia retusa*. *J Asian Nat Prod Res* 2011;**13**:75–9.
11. Bach SM, Fortuna MA, Attarian RD, de Trimarco JT, Catalán CA, Av-Gay Y, et al. Antibacterial and cytotoxic activities of the sesquiterpene lactones cincin and onopordopicrin. *Nat Prod Commun* 2011;**6**:163–6.
12. Geroushi A, Auzi AA, Elhwuegi AS, Elzawam F, Elsherif A, Nahar L, et al. Antiinflammatory sesquiterpenes from the root oil of *Ferula hermonis*. *Phytother Res* 2011;**25**:774–7.
13. Jin JH, Lee DU, Kim YS, Kim HP. Anti-allergic activity of sesquiterpenes from the rhizomes of *Cyperus rotundus*. *Arch Pharm Res* 2011;**34**:223–8.
14. Xiao Y, Zheng Q, Zhang Q, Sun H, Guéritte F, Zhao Y. Eudesmane derivatives from *Laggera pterodonta*. *Fitoterapia* 2003;**74**:459–63.
15. Wei JX, Zhao AH, Hu JL, et al. Constituents of *Laggera pterodonta*. *Acad J Kunming Med Coll* 1995;**16**:83–4.
16. Yang GZ, Li YF, Yu X, Mei ZN. Terpenoids and flavonoids from *Laggera pterodonta*. *Acta Pharm Sin* 2007;**42**:511–5.
17. He XM, Carter DC. Atomic structure and chemistry of human serum albumin. *Nature* 1992;**358**:209–15.
18. Stock RS, Ray WH. Interpretation of photon correlation spectroscopy data: a comparison of analysis methods. *J Polym Sci Part B* 1985;**23**:1393–447.
19. Eftink MR. Fluorescene quenching reactions: probing biological macro-molecular structures. In: Eewey TG, editor. *Biophysical and biochemical aspects of fluorescence spectroscopy*. New York: Plenum; 1991. p. 1–41.
20. Yang P. *An introduction to bioinorganic chemistry*. Xi'an: Xi'an Jiaotong University Press; 1991. p. 163–4.
21. Lakowicz JR, Weber G. Quenching of fluorescence by oxygen. A probe for structural fluctuations in macromolecules. *Biochemistry* 1973;**12**:4161–70.
22. Ni Y, Liu G, Kokot S. Fluorescence spectrometric study on the interactions of isoprocarb and sodium 2-isopropylphenate with bovine serum album. *Talanta* 2008;**76**:513–21.
23. Hu YJ, Liu Y, Sun TQ, Bai AM, Lü JQ, Pi ZB. Binding of anti-inflammatory drug cromolyn sodium to bovine serum album. *Int J Biol Macromol* 2006;**39**:280–5.
24. Zhang G, Chen X, Guo J, Wang J. Spectroscopic investigation of the interaction between chrysin and bovine serum albumin. *J Mol Struct* 2009;**921**:346–51.
25. Ross PD, Subramanian S. Thermodynamics of protein association reactions: forces contributing to stability. *Biochemistry* 1981;**20**: 3096–102.
26. Chen G. *Fluorescence analysis*, 2nd ed., Beijing: Science Press; 1990.
27. Wang YQ, Tang BP, Zhang HM, Zhou QH, Zhang GC. Studies on the interaction between imidacloprid and human serum albumin: spectroscopic approach. *J Photochem Photobiol B* 2009;**94**: 183–90.
28. Murphy RM. Static and dynamic light scattering of biological macromolecules: what can we learn? *Curr Opin Biotechnol* 1997;**8**: 25–30
29. Nobbmann U, Connah M, Fish B, Varley P, Gee C, Mulot S, et al. Dynamic light scattering as a relative tool for assessing the molecular integrity and stability of monoclonal antibodies. *Biotechnol Genet Eng Rev* 2007;**24**:117–28.
30. Yu M, Ding Z, Jiang F, Ding X, Sun J, Chen S, et al. Analysis of binding interaction between pegylated puerarin and bovine serum albumin by spectroscopic methods and dynamic light scattering. *Spectrochim Acta A Mol Biomol Spectrosc* 2011;**83**:453–60.
31. Barbosa S, Taboada P, Mosquera V. Analysis of the interactions between human serum albumin/amphiphilic penicillin in different aqueous media: an isothermal titration calorimetry and dynamic light scattering study. *Chem Phys* 2005;**310**:51–8.